# Mechanism of Coarsening and Bubble Formation in High-Genus Nanoporous Metals

J. Erlebacher

*Johns Hopkins University, Department of Materials Science and Engineering,*
*3400 North Charles Street, Baltimore, Maryland 21218, USA*
(Received 30 March 2011; published 3 June 2011)

Coarsening of crystalline nanoporous metals involves complex changes in topology associated with the reduction of genus via both ligament pinch-off and void bubble formation. Although void bubbles in metals are often associated with vacancy agglomeration, we use large-scale kinetic Monte Carlo simulations to show that both bubble formation and ligament pinch-off are natural results of a surface-diffusion-controlled solid-state Rayleigh instability that controls changes in the topology of the porous material during coarsening. This result is used to find an effective activation energy for coarsening in nanoporous metals that is associated with the reduction of topological genus, and not the reduction of local surface roughness.

Nanoporous metals with bicontinuous open porosity containing ligament and void diameters of order 10 nm are made via a pattern-forming instability when the selective electrochemical dissolution rate of one component of a two-component ideal solid solution is of the same order as the rate of surface diffusion of the remaining alloy component (''dealloying'') [1]. For instance, in the dissolution of Ag from $Ag_{65}Au_{35}$ to make nanoporous gold, gold atoms diffuse along the solid-electrolyte interface during dissolution and reconfigure themselves into an extended three-dimensional porous material whose crystallinity (the size of single-crystal domains) matches the crystallinity of the parent material; this is usually many orders of magnitude larger than any pore or ligament diameter [2,3]. The question of how these materials coarsen, evolving toward the equilibrium Wulff shape, has been of practical interest to tune length scale and shape in order to optimize nanoscale-related optical, electromechanical, and catalytic properties [4–6]. The primary model used or morphological coarsening of nanoporous metals has been the classical surface-diffusion-controlled smoothening model developed by Herring in which a characteristic length, e.g., ligament diameter, is tracked as a function of time and temperature [7,8]. We show here that the application of this model to coarsening of nanoporous metals must be considered carefully, as shape evolution is controlled not by the smoothening of high curvature surface regions, but rather by topological genus-decreasing events (ligament pinch-off and void bubble formation) manifested as solid-state Rayleigh instabilities.

To study coarsening, kinetic Monte Carlo (KMC) simulations were performed on simulated dealloyed nanoparticles with radii up to 100 atoms ($\sim 40$ nm diameter particles) generated using methods described in Ref. [9]. Nanoparticles were chosen because they are easy to visualize and there is also recent interest in the catalytic activity of nanoporous nanoparticles toward important reactions in

energy technologies [10,11]. In addition, the accessible system size was essentially bulk, i.e., large enough to avoid having to include any truly nanoscopic Gibbs-Thomson effects such as a melting point depression. Briefly, our KMC technique (MESOSIM) places a system of atoms at assigned sites on a three-dimensional face-centered cubic lattice according to an input composition, and then evolves the system according to the following standard repeated rules [12]: (a) if there are $n$ transitions (diffusion or dissolution events) that can occur in a particular iteration, indexed by $i$, and each transition occurs at a rate $k_i$, then the probability of a particular event occurring will be $P_i = k_i / \sum k_j$; (b) as all events are occurring in parallel and any one event will occur over some increment of time according to a Poisson distribution, the time step is incremented by $\Delta t = -\ln \xi / \sum k_j$, where $\xi$ is a random number in (0,1]. The KMC model used here takes atoms that are completely coordinated out of memory, bookmarking their neighbors, so the system size scales as the surface area of the structure. This surface area includes all undercoordinated atoms, including the near neighbors of vacancy point defects. Transition rates for diffusion were assigned according to a bond-breaking model for which a transition from an $N$-coordinated site was given by $k = \nu \exp(-NE_b/k_BT)$, where $E_b = 0.15$ eV for all bond energies and $\nu = 10^{13}$ $sec^{-1}$ was the attempt frequency; these values led to dynamics of coarsening that roughly matched experimental values for the nanoporous gold system, although it is emphasized that this is a qualitative correspondence. Typical simulation runs ran for $4 \times 10^{10}$ iterations. A fully dealloyed porous nanoparticle with a roughly 100-atom radius corresponds to a nonvoid volume of $\sim 7.5 \times 10^5$ atoms.

Figure 1 shows representative data: a simulated dealloyed particle, here of an initial sphere with radius $r = 100$ atoms, and its time evolution as it coarsens toward the Wulff shape at temperatures of 300, 600, 900, and
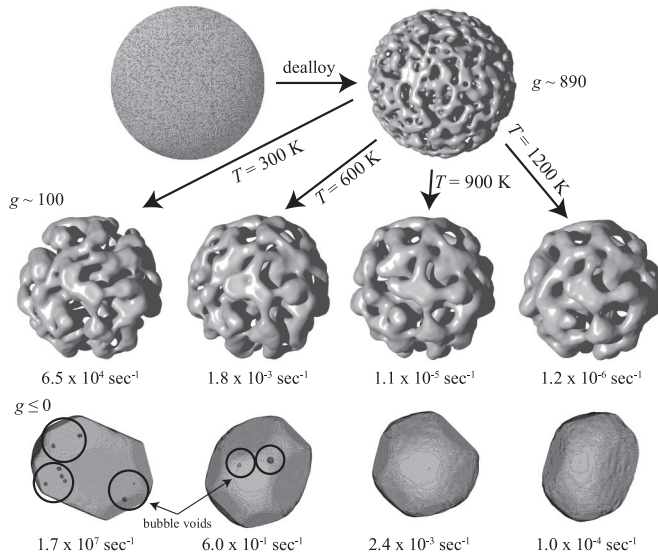
FIG. 1.   Simulated evolution of nanoporosity and bubble voids during coarsening, showing snapshots of a high topological genus nanoporous nanoparticle as it evolves toward the Wulff shape at different temperatures (in columns). Top row: initial conditions. Middle row: intermediate genus structures ($g \sim 100$) at 300, 600, 900, and 1200 K, with corresponding coarsening times. Bottom row: final coarsened structures ($g \leq 0$) at the same temperatures, and corresponding coarsening times. Obvious bubble voids in the final structures are circled. For clarity, only the front half of the triangulated mesh in the $g \leq 0$ row is illustrated; opaque triangles are rendered in the higher genus images using ray-tracing software (POV-RAY). The scale of individual atoms in the undealloyed initial condition ($r = 100$) is shown for reference.

1200 K. In order to separate effects of coarsening (the focus of this Letter) from dissolution, the initial dealloyed structure has been turned into a single component, and the time reset to $t = 0$. The concentration of vacancies in the initial porous structures is quite high—approximately 0.2%. This high concentration reflects the nonequilibrium conditions of porosity evolution and the high driving force for dissolution relative to surface diffusion. For comparison, energetic considerations for the formation energy of vacancies calculated as an ideal solution give the equilibrium fraction rising from $7.6 \times 10^{-16}$ at 300 K to only $1.7 \times 10^{-4}$ at 1200 K. During coarsening at temperatures below 900 K, "bubbles" always appear inside the ligaments, i.e., nonconnected voids whose diameter is smaller than the diameter of any ligaments in which they reside, but still containing volumes sometimes many thousands of atoms large. The term bubble contrasts these geometric features both from the void channels of the primary dealloyed structure, which are connected in the bicontinuous geometry and have diameter approximately equal to the average ligament diameter [13,14], and vacancies (12-coordinated point defects).

The observation of a nonequilibrium concentration of vacancies is suggestive of a mechanism of bubble formation by vacancy agglomeration via bulk diffusion. In fact,
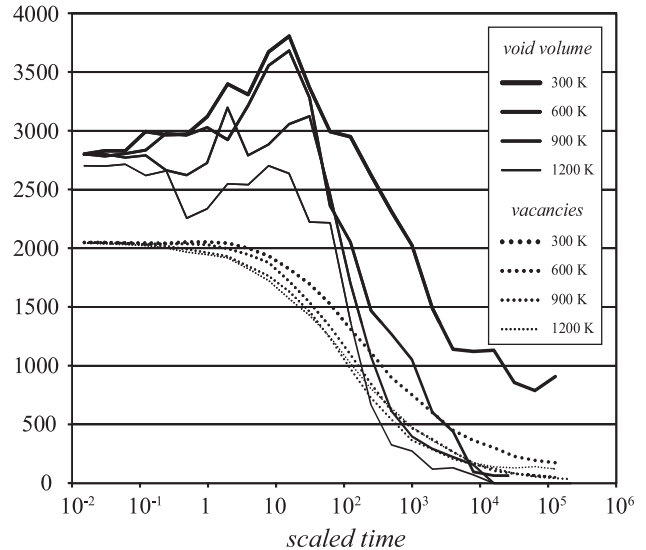


FIG. 2.   Void bubble and vacancy evolution in the simulated particles of Fig. 1, versus scaled time $t' = t\nu e^{-6E_b/k_B T}$ at 300, 600, 900, and 1200 K. Solid lines: integrated volume of void bubble; dotted lines: total number of vacancies.

an old model for porosity evolution, due to Pickering and Wagner, invoked the possibility that silver atoms from the bulk are drawn toward the electrolyte via a "divacancy" mechanism where diffusion of two-vacancy clusters is driven simply by the silver concentration gradient between the Ag-poor porous region and the Ag-rich bulk [15]. However, any bulk vacancy mechanism is too slow at room temperature to account for the rate of porosity evolution, and this model has largely been superseded by a surface-diffusion-controlled model in which porosity evolution is controlled by the rate at which gold atoms diffuse with receding step edges rather than being left behind as a nonequilibrium supersaturated adatom lattice gas when silver in terraces is attacked by an electrolyte [2]. Nonetheless, Rosner *et al.* recently made the surprising discovery that the ligaments of nanoporous gold are riddled with bubbles whose diameters were sometimes a significant fraction of the ligament size, reviving attention in the bulk-diffusion divacancy mechanism of porosity evolution [16].

In the simulation context, the idea that bubble formation is due to bulk diffusion and agglomeration of point defects is wrong. Figure 2 illustrates how the number of vacancies and the integrated bubble volume change with time. First, the total bubble volume increases for a period of time in which the number of vacancies is roughly constant. During this time period, there could be a formation rate of vacancies that matches an annihilation rate associated with coalescence into a bubble that leads to a steady-state concentration, but then one would expect this steady-state concentration to be approximately equal to the equilibrium concentration. However, Fig. 2 also shows that after the initial transient, the number of vacancies clearly decreases over the course of the simulation and does not ever reach

the equilibrium value except for simulations at 1200 K. These observations indicate that at low temperature, the mobility of vacancies is slow over the time scales of both coarsening and bubble formation—a reasonable conclusion. Indeed, inspection of the position of vacancies at the end of the low-temperature simulation shows they are anisotropically distributed through the structure, a reflection of their low mobility in the bond-breaking model used for simulation kinetics.

We now argue that bubbles are formed naturally during surface-diffusion-controlled coarsening, and are topologically complementary to ligament pinch-off. Coarsening in nanoporous metals is driven by reduction of the overall surface energy, and proceeds by surface-diffusion currents proportional to gradients in the local surface chemical potential. Herring [8] primarily considered the case where surface-diffusion currents lead to surface flattening of convexities and concavities; this is the relevant case for thin film growth. In porous metals, however, coarsening proceeds also by ligament pinch-off in which surface diffusion pulls material away from saddle-point curvature ligaments, which thin to one atom thick and then break. In contrast to surface flattening, ligament pinch-off has the geometric effect of reducing the topological genus $g$. The genus is a measure of how many handles a geometric structure has— for instance, a coffee cup and a torus are topologically equivalent with genus $g = 1$, as they can be deformed one into the other without cutting any ligaments. A sphere has genus $g = 0$. Bubbles reduce the topological genus of the structures in which they reside. For instance, a bubble inside a sphere has genus $g = -1$. Generally, in terms of the number of handles $n_h$ and bubbles $n_b$, the genus is given by $g = n_h - n_b$ [17]. The genus of surface with well-defined "inside" and "outside" surfaces, such as the simulated structures here, is easily measured by converting the surface into a triangulated mesh, and then using the Poincaré formula $2 - 2g = n - e + f$, where $n$ is the number of mesh nodes, $e$ the number of edges, $f$ the number of faces, and $2 - 2g$ is the so-called Euler characteristic. The $r = 100$ simulations began with $g \sim 890$ and this value decays to below zero over the course of any simulation.

The kinetics of ligament pinch-off are controlled by Rayleigh instabilities. The typical Rayleigh instability problem analyzes a cylinder of radius $R_0$, whose radius is perturbed by an instability of wavelength $\lambda$ [18]. For wavelengths longer than a critical $\lambda_{\text{crit}}$, the amplitude will grow because the total surface energy of system decreases; ultimately, the cylinder breaks up into a series of droplets. Because only surface energy considerations enter into the argument, the construction is symmetric with regard to which phase is solid and which is void, and thus applies to void cylinders as well; i.e., these should break up into a series of bubbles. Apply these ideas to open porosity dealloyed metals: because all void space is connected, the structure should be seen as a network of both solid cylinders and void cylinders, and thus it is natural that Rayleigh

instabilities should lead to both ligament pinch-off and bubble formation. There is, however, an important asymmetry between ligament pinch-off and bubble formation; namely, once a bubble is formed, it is separated from any mass transport paths that can lead to further morphological evolution whereas pinched-off ligaments are still connected to the entire primary external surface of the structure (one caveat: "droplets" occasionally do become disconnected from the primary structure via ligament pinch-off, but these are rare compared to bubbles).

In the cylindrical Rayleigh instability with mass transport controlled by surface diffusion, the time constant for an unstable mode to grow is given by $\tau^{-1}(\lambda) \propto (4\pi^2 \gamma / R_0^2 \lambda^2)[1 - (2\pi R_0/\lambda)^2]$, where $\gamma$ is the surface energy [18]. For the case of the nanoporous metal, we show below that it is a reasonable ansatz that the characteristic length of porosity (length of any ligament) at any time is some multiple of the high radius principal curvature of the ligament. In this case, $R_0 \sim m\lambda$, $m > 1$, so we expect the time $\tau_{\text{PO}}$ for a ligament to pinch-off to go as $\tau_{\text{PO}} \sim \lambda^4$. These observations explain the peak in the number of bubbles versus time (Fig. 2). At short times, bubbles are being formed because all characteristic lengths are small, so their number increases. However, once formed, these bubbles are stagnant because the characteristic length of the structure is always larger than any void. Ligaments, in contrast, are never stable, and ligament pinch-off can destroy nearby bubbles; thus, over longer times the number of bubbles decreases.

To quantify this picture, we identify two characteristic lengths. The first, suggested by Mendoza et al., is the (volume per genus)/(surface area per genus) [17]; here the bounding volume of a sphere completely enclosing the particle for each simulation is found to be approximately constant, varying <5% over any run, so $\lambda_1 \sim 1/A$. A second length is the average ligament radius, which can be found through the average mean curvature, i.e., $\lambda_2 \sim \langle(\kappa_1 + \kappa_2)/2\rangle^{-1}$, where $\kappa_1$ and $\kappa_2$ are the principal radii of curvature at each node, and each node is weighted by its Voronoi area in the average. To make the calculation of $A$ and each $\kappa$, we used a smoothening algorithm in which the triangulated mesh of surface atoms is smoothened in such as way as to simultaneously preserve as closely as possible the overall volume and the genus as calculated by the Gauss-Bonnet theorem rather than the Poincaré theorem. Details of this calculation will be presented elsewhere.

Figure 3 shows the time decay of the normalized inverse lengths $\lambda_1$, $\lambda_2$ and the normalized genus. The equivalence of $\lambda_1$ and $\lambda_2$ justifies the above ansatz regarding the ligament diameter compared to the characteristic length of porosity. Note that the rate of surface area reduction always lags the rate of change of genus. These characteristics are indicative of a coarsening process that progresses by a series of localized pinch-off events nearby each of which the local curvature distribution deviates significantly from the average curvature distribution of the system
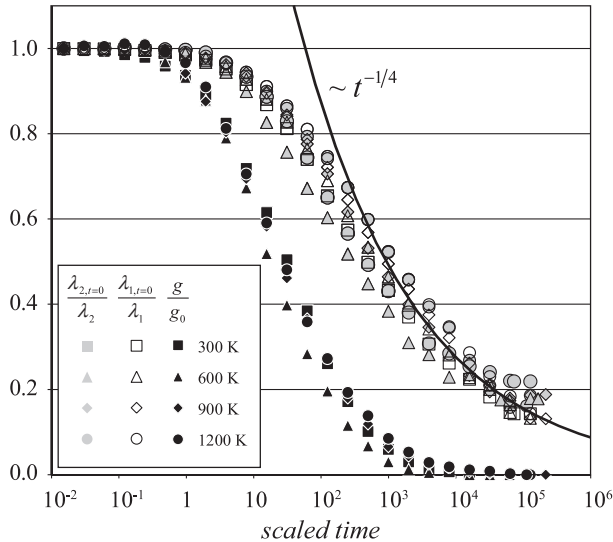
FIG. 3.   Time evolution of topological measures of nanoporous particles versus scaled time $t' = t\nu e^{-6E_b/k_B T}$: (solid black symbols) normalized genus $g/g_0$; (open symbols) normalized surface area $A/A_0$; (gray symbols) normalized average mean curvature. The symbol shape corresponds to the simulation temperature: squares (300 K), triangles (600 K), diamonds (900 K), and circles (1200 K). For reference, a classical $t^{-1/4}$ decay of the characteristic length scale is shown; note that classical scaling only begins at a scaled time of $10^3$ sec$^{-1}$, when the genus approaches zero.

because of the extra mass that remains right near the pinch-off point. Herring showed that structures undergoing self-similar coarsening should exhibit a power-law scaling $\lambda \sim t^{-1/4}$ between any characteristic length $\lambda$ and coarsening time $t$ [8]. But to remain a self-similar structure, an assumption underlying Herring's analysis, the local thickening of material near a pinch-off point must be redistributed over the entire structure prior to the next pinch-off event, so that the average ligament diameter everywhere grows. However, long range surface diffusion (surface flattening) and ligament pinch-off both operate over times that scale as $\lambda^4$, so self-similar coarsening is impossible unless the genus has essentially collapsed and the ligaments are gone, i.e., when $g \sim 0$, as seen. This behavior is highly pronounced in the finite-radius particle simulations here. Indeed, for topologically complex materials, it has been suggested a test of self-similarity is that the product $g_v \lambda^3$ is time independent, where $g_v$ is the genus per volume and $\lambda$ is any characteristic length. We find (not shown) that this product is constant only for short times at low temperatures.

As the surface area response always lags the reduction of genus due to Rayleigh instabilities, we conclude ligament pinch-off controls coarsening in nanoporous nanoparticles. This can be tested by examination of the functional dependence of the genus decay as it varies with temperature. Assuming there is a universal genus decay function, simple dimensional and kinetic considerations suggest that the genus function is of the form $g = g(kt)$, where $k$ is a

transition frequency; in turn, the simplest model for this frequency has Arrhenius dependence, i.e., $k = \nu e^{-Q^*/k_B T}$, where $Q^*$ is an "activation energy" for pinch-off. We can find $Q^*$ by plotting $g(t')$ vs $t' = kt$. If this construction has merit, a single value of $Q^*$ should data collapse of all genus vs time data. Such scaling has been used to present all time-dependent data in this Letter. Figure 3, in particular, shows excellent data collapse for the normalized genus when using an activation barrier of $Q^* = nE_b$ with $n = 6.0$; obvious deviation from collapse is seen even when the prefactor $n$ deviates by 0.1. This value for $n$ is physically reasonable, and could correspond to a number of geometric configurations associated with pinch-off, including an atom bounded on either side by (111) oriented microterraces. In contrast, the best data collapse for the characteristic length (not shown) has $n = 5.8$, which would lead to an inferred value of $E_b$ of 0.16 eV, which does not correspond to any microscopic bond energy. We concede this is only a small deviation from the correct value, but still a source of error.

In conclusion, the coarsening mechanism of nanoporous single-crystal metals is controlled by ligament pinch-off associated with Rayleigh instabilities, and this also leads to bubble formation. The results here have implications for the interpretation of coarsening experiments of nanoporous metals, namely, to find an activation energy that corresponds to microscopic pinch-off events, examine the topological genus versus time and temperature (for instance, by making a triangulated mesh from the surface measured using transmission electron microscopy tomography) and not only surface area decay.

[1]   J. Erlebacher et al., MRS Bull. **34**, 561 (2009).
[2]   J. Erlebacher et al., Nature (London) **410**, 450 (2001).
[3]   S. Van Petegem et al., Nano Lett. **9**, 1158 (2009).
[4]   X. Y. Lang et al., Appl. Phys. Lett. **94**, 213109 (2009).
[5]   S. Parida et al., Phys. Rev. Lett. **97**, 035504 (2006).
[6]   A. Wittstock et al., Science **327**, 319 (2010).
[7]   L. H. Qian and M. W. Chen, Appl. Phys. Lett. **91**, 083105 (2007).
[8]   C. Herring, J. Appl. Phys. **21**, 301 (1950).
[9]   J. Erlebacher, J. Electrochem. Soc. **151**, C614 (2004).
[10]  I. Dutta et al., J. Phys. Chem. C **114**, 16309 (2010).
[11]  M. Shao et al., J. Am. Chem. Soc. **132**, 9253 (2010).
[12]  C. C. Battaile, D. J. Srolovitz, and J. E. Butler, J. Appl. Phys. **82**, 6293 (1997).
[13]  T. Fujita et al., Appl. Phys. Lett. **92**, 251902 (2008).
[14]  Y.-C. Chen et al., Appl. Phys. Lett. **96**, 043122 (2010).
[15]  H. W. Pickering, C. Wagner, J. Electrochem. Soc. **114**, 698 (1967).
[16]  H. Rosner et al., Adv. Eng. Mater. **9**, 535 (2007).
[17]  R. Mendoza et al., Acta Mater. **54**, 743 (2006).
[18]  R. W. Balluffi, S. M. Allen, and W. C. Carter, *Kinetics of Materials* (John Wiley & Sons, New York, 2005), p. 345.